Decane droplet combustion onset in air behind a Mach 5.3 shock wave

Florent VIROT, Alain CLAVERIE
Institut PPRIME UPR 3346 CNRS
Chasseneuil du Poitou, 86360, France

1 Introduction

Liquid fuels are key to transport applications as their combustion releases high energy and their density provides low-volume storage. Early liquid fuel detonation studies were done in 1960's where combustion instabilities evaluation in rocket combustion chamber was of primary importance [1]. Since then, several experiments were carried out and models were proposed for liquid fuel systems in oxygen atmosphere. These studies focused on spray detonation and isolated droplet interaction with a shock wave in incident or reflected shock tube configuration. But very little experimental work has been devoted to the interaction between an incident shock wave and a fuel droplet in air such as in Lu et al's work [2]. Contrary to oxygen enriched atmophere, the latter had performed heptane-air experiments where only a deflagrative mode of combustion is observed in the wake of the single shocked fuel droplet without any blast wave. The small number of studies may be explained by the fact that the smaller the droplet diameter, the more difficult it is to observe ignition: Pinaev and Sichev took 3-mm drop in oxygene atmosphere since signal luminosity is more than one order of magnitude less with 1-mm drop [3]. The deformation and aerobreakup of isolated liquid fuel have been recently published but the ignition was not reported.

Development of airbreathing engines such as scramjet or rotative detonation chamber will need fundamental understanding of how liquid fuel mix with air and burn behind a shock wave. The purpose of this paper is to experimentally observe where and when isolated decane droplets burn behind a shock wave that propagates at Mach number M_s=5.3 ie in the conditions close to those of a gaseous premix stœchiometric decane/air detonation front.

2 Experimental setup

A $92-\mathrm{mm}$-inner-diameter detonation driven shock tube is used as in previous works [4]. The tube is connected to a $80\,\mathrm{mm}\times80\,\mathrm{mm}$-squared-cross-section chamber with optical access through a $150\,\mathrm{mm}$ round to square transition section. Dimensions are reported on the Fig. 1. Two optical setup are used: a schlieren configuration and a direct visualisation configuration. Both configurations have an additional still camera in order to get accurate measurements of droplet diameter with a resolution of around $383\,\mathrm{pxl/mm}$ a pulsed light source backlights the scene (about $7.8\,\mathrm{mm}$ by $10.8\,\mathrm{mm}$) which is observed

Correspondence to: florent.virot@ensma.fr

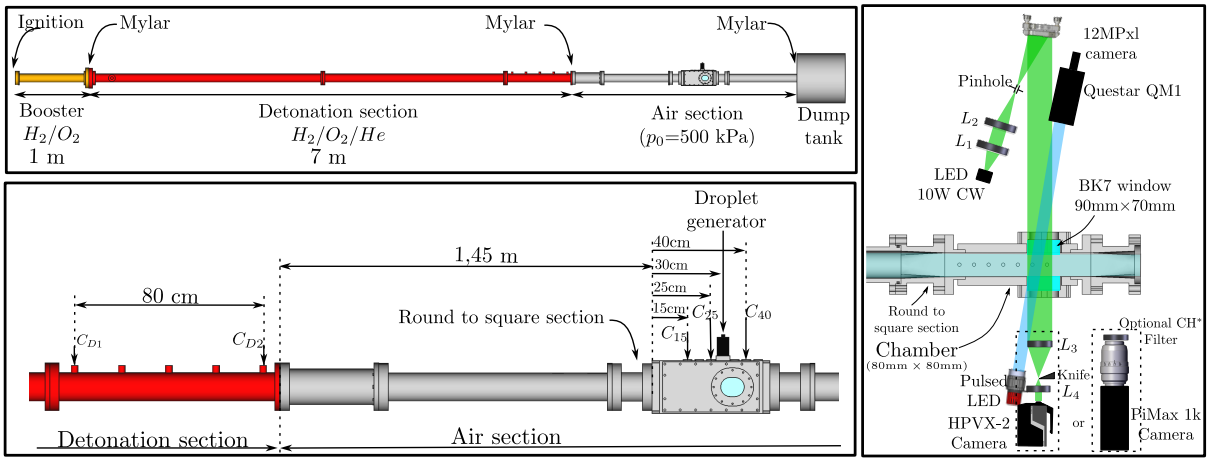

Figure 1: Experimental setup. Left: Detonation driven shock tube (side views). Right: Optical configurations (top view).

on a 12 Mpxl CCD sensor with a Questar QM1 long microscope objectiv lens attached. Experiments with schlieren are processed with a Shimadzu HPVX-2 ultra high speed camera with a 10 W continuous green LED as light source; the frames of 400×250 pixels correspond to a 21.7 mm×13.6 mm field of view for shots #W and #1 and 12.8 mm×8 mm for shot #2 and #3). Direct visualisation experiments are performed with HPVX-2 for shot #4 (by switching off the light and removing the knife of the schlieren configuration, same field of view as shot #2) and with an 1024×1024 pxl intensified camera Princeton PiMAX 1K that gives 17.3 mm×17.3 mm field of view with a Nikon 200 mm lens. A filter (SemRock FF01-445/45) is added in the last experiment (shot #7) which transmits 90% of the wavelengths around 445 nm (45 nm bandwidth); this allows to record CH* spontaneous emission, taken into account any potential broadening of the spectra due to pressure effect.

A TSI MDG100 droplet generator creates a continuous train of monodisperse droplets; it is fed of decane (except one shot with water) by an homemade syringe pump. Parameters used in this work lead to droplet size d_g ranging between 145 µm and 180 µm. The experimental conditions are summarized in Table 1 where $t_r = \frac{d_g}{u_1}\sqrt{\frac{\rho_l}{\rho_1}}$ and $We = \frac{\rho_1 u_1^2 d_g}{\sigma}$ stand for the Rayleigh characteristic time and the Weber number respectively. The surface tension taken is σ=23.83 mN/m for decane (72 mN/m for water) although density is ρ_l=700 kg/m^3 for decane (1000 kg/m^3 for water).

Five Kistler 603B pressure sensors are mounted on the detonation tube and on the chamber in order to

Table 1: Summary of experimental conditions.

Shot number	D m/s	M$_s$ –	d_g µm	t_r µs	We –	Comments / Optical configuration S=schlieren ; DV=direct visualisation,
#1	1817	5.34	160	1.54	52781	S, HPVX-2, 2 MHz, t_{expo}=200 ns
#2	1817	5.34	160	1.54	52781	S, HPVX-2, 5 MHz, t_{expo}=110 ns
#3	1816	5.22	148	1.48	45109	S, HPVX-2, 2 MHz, t_{expo}=200 ns, N_2
#4	1806	5.30	145	1.41	47025	DV, HPVX-2, without filter, 1 MHz, t_{expo}=700 ns
#5	1800	5.27	175	1.71	55930	DV, PiMAX1K, without filter 6 µs gate
#6	1831	5.37	175	1.67	58713	DV, PiMAX1K, without filter 10 µs gate
#7	1828	5.36	180	1.72	60123	DV, PiMAX1K, with SemRock filter, 10 µs gate
#W	1791	5.24	178	2.05	18550	S, HPVX-2, 2 MHz, t_{expo}=200 ns, WATER

monitor the detonation pressure profils and the shock wave in air in the chamber. Pressure signal are recorded on a National Instrument PXI-5105 digital oscilloscope at $10\,\mathrm{MHz}$ and one of which serves as a trigger signal for the cameras.

The detonation tube is operated with stœchiometric H_2/O_2/He and H_2/O_2 mixtures in the detonation and booster sections respectively. Initial pressure and composition are ajusted to generate a shock wave that propagates in air at Mach number 5.3 at $500\,\mathrm{kPa}$. This device have proved highly reproducible.

3 Results

3.1 General overview of the shock/droplet interaction

Fig. 2 presents a selection of frames showing the interaction of the shockwave at Mach number 5.3 with droplets. Frames on the left and on the center columns show the evolution of decane droplets in shot #1 and shot #3 respectively while, on the right column, droplets are made of water (shot #W). Shot #3 has a smaller field of view than shot #1. Shots #W and #3 are inert cases since on one hand it is a water droplet in air atmosphere and, on the other hand, it is a decane droplet in pure nitrogen atmosphere.

Droplets produced in #3 and #W are very regular in both drop diameter and spacing between the droplets while #1 has shown some irregularities in spacing. Various dimensionless times T are selected for comparison up to T=8 in that figure. Thus, according to individual Rayleigh time, the absolute times differ for every row. In every experiment, one can identify the straight incident shockwave. As soon as the latter hits the droplets, an attached bow shock appears immediately on every droplet due to the velocity lag between the supersonic flow behind the shock and the droplet nearly at rest.

At T=1, aerodynamic forces acting on droplets cause them to deform into a prolate ellipsoid which height is three times the initial diameter. The shear flow generates a very fine mist which is entrained at a velocity close to that of the flow. The mist that skirts arount the drop appears black on the image as the collimated rays are trapped; thus, the process inside the mist is totally hidden with this visualization technique. Shapes are very similar between water or decane droplet except that in the decane case, the tails appear bright. These tails extend and widen over the time and appear increasingly turbulent. The density of droplet and its surrounding mist diminish over the time (through processes such as stripping and evaporation) which can be observed with dark areas becoming smaller and smaller. As droplet moves, the bow shock progressively straightens, detaches when $T \approx$4 for decane droplet (or $T \approx$5 for water droplet) and moves away.

Compared with the water droplet case, the decane droplet cases typically show shorter times to obtain a "translucent" mist and this mist offers less position variations along x axis (looking at the leading edge, on the left of the droplet) despite any irregular droplet spacing that can occur initially in the jet as in #1.

3.2 Leading edge evolution

The leading edge path of the droplet is manually tracked over the time for minimum, mean and maximum droplet displacement at each time. Results are plotted in Fig. 3 where the reference time is set at the moment when the shock wave touches the droplet. Each curve shows a parabolic evolution of the displacement at the beginning, indicating that the acceleration of the droplet is constant. On longest times, the displacement is linear meaning that the velocity is constant and is about $1320\,\mathrm{m/s}$ (roughly 88% of the post shock air flow velocity). Due to the slight variation in droplet diameter from one experiment to another and the different properties between decane/water, displacements of decane droplets separates from water ones after $10\,\mu\mathrm{s}$; however, in dimensionless space (plot on the right), all the curves are superimposed. Moreover, the fit curve $X = 3/8 C_d T^2$ agrees well with the data in the parabolic part of displacements (ie. for $T \leq 4$).

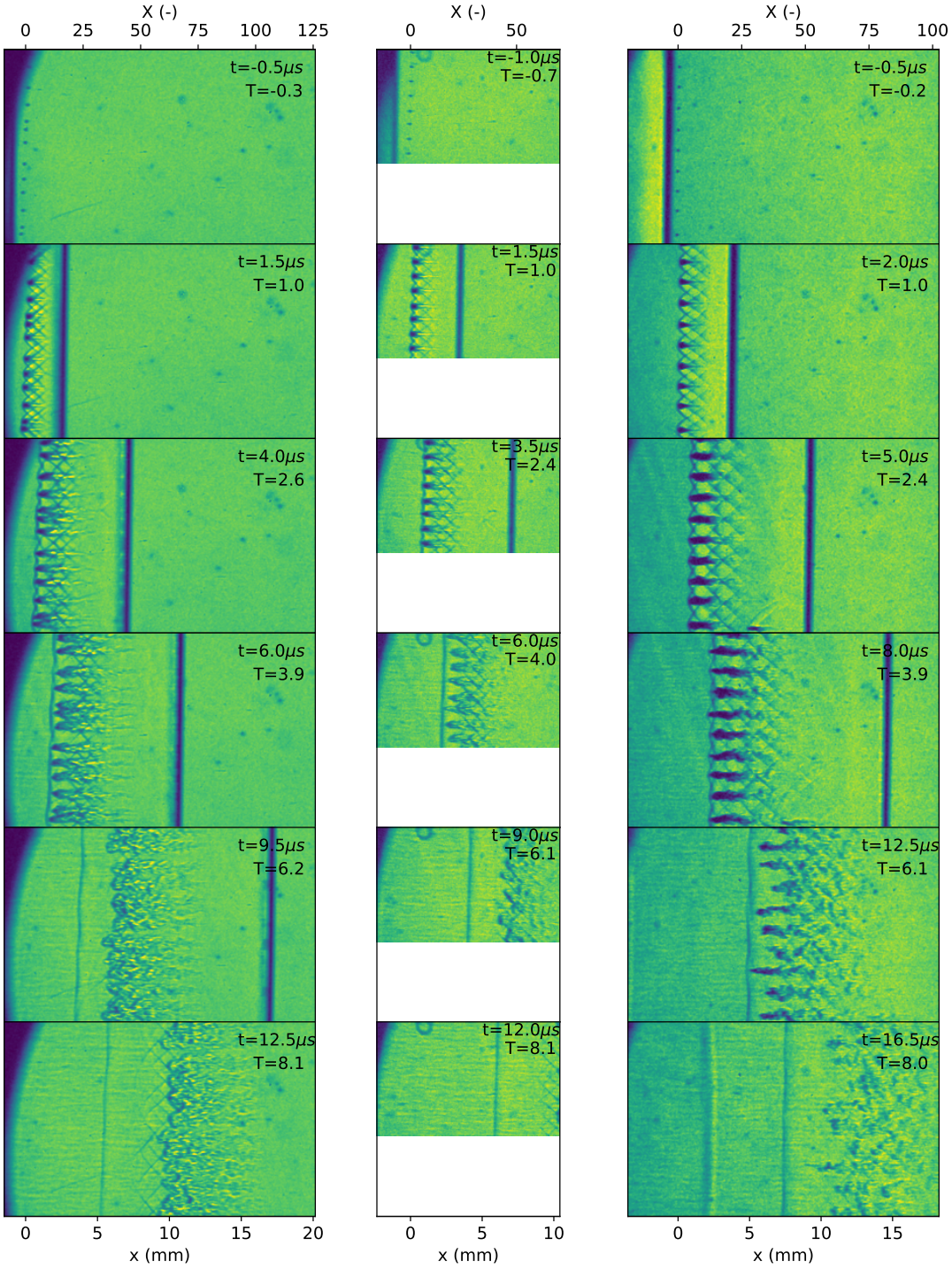

Figure 2: Evolution of the droplets during the passage of the shock wave at M_s=5.3. Left: shot #1 with decane droplets in air. Center: shot #3 with decane droplet in pure N_2 atmosphere. Right: shot #W with water droplet in air.

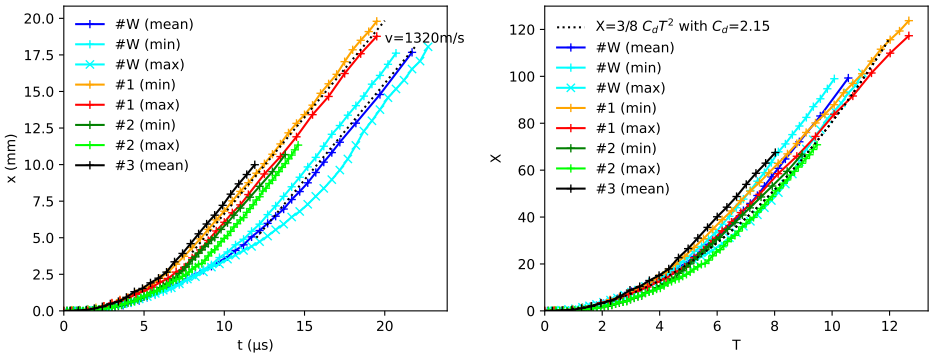

Figure 3: Evolution of the droplet displacement with time. Left: absolute time t and displacement x. Right: Dimensionless time T and displacement X

According to these results, there is no dramatic difference between inert cases (decane/N_2 and water/air) and a reactiv case. Thus, this leave us to wonder if chemical reactions really occur. Though, a constant pressure reactor calculations indicates that a decane/air reaction should take place in less than $3\,\mu s$. The following section aims to answer this question.

3.3 Inflammation evidence

Experiments with direct visualization technique are conducted. The high speed HPVX-2 camera running at $1\,MHz$ with long exposure time ($700\,ns$) reveals very low luminous signals difficult to interpret alone. Switching to PiMAX 1K intensified camera gives the images displayed on Fig.4.

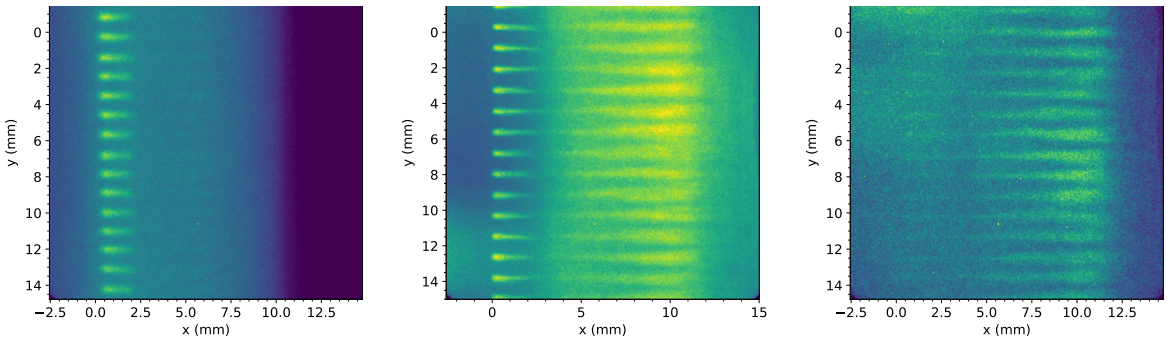

Figure 4: Direct visualization using an intensified camera. Left: short $6\,\mu s$-long integration gate. Center: $10\,\mu s$-long integration gate. Right: $10\,\mu s$-long integration gate with CH^* filter.

Without CH^* filter, the droplet positions can be trustly assumed to be where high luminous area are observed; indeed, similar shapes can be recognized from schlieren experiments. With filter, these high luminous area disappear and the x-axis position is determined from the jet position recorded before the test. On the short $6\,\mu s$-long gate test, the shock wave position can be identified at x=$10\,mm$ as the background corresponding to postshock state is more luminous while in long gate tests the shock wave has swept all the field of view. Both $10\,\mu s$-long gate tests reveals luminous signal in the wake of the droplets which can serve as the droplet position determination on the y-axis.

The long gate test with CH^* (right image on Fig. 4), shows where chemical reactions take place. It is found that CH^* signals is mainly present in the wake of the droplets and about $5\,\mu s$ after the shock passage. CH^* signal is very low – yet not zero – around the droplet but it may be also possible that the mist hides at least half the luminous emission behind it. Besides, it means that the high luminous

areas around the droplet are produced by wavelengths above $468\,\mathrm{nm}$. Supplementary study is needed to understand their origin and to determine, in particular, if it could come from the detonated burned gas light illuminating the droplets from visible to infrared spectrum.

Finally, shot #4 post-processing through the light of previous conclusions gives the Fig. 5 where averaging y-axis pixel intensities results of an 1D-array for every frame. Droplet leading edge, both beginning and end of the wake are reported from shot #1 and dimensionless variables are calculated with average diameter. Shock wave passage can be identified on the plot (but long exposure time returns a spread signal) which matches to shock wave position of shot #1. Light signal around the drop is observed up to $4\,\mu\mathrm{s}$, the one from the wave starts $7\,\mu\mathrm{s}$ after shock passage on the droplet.

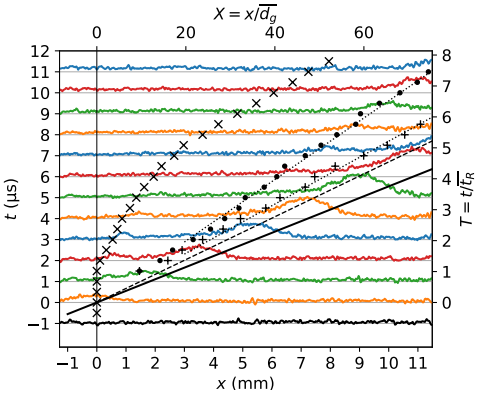

Figure 5: Luminous signal from shot #4 plotted with data of shot #1: shock wave position (solid line), postshock fluid velocity (dash line), droplet leading edge (marker x), beginning of the wake (marker o) and end of the wake (marker +).

4 Conclusion

Experiments have been carried out in order to detect where and when chemical reactions occur when a shock wave impacts a decane droplet 150–$180\,\mu\mathrm{m}$ in diameter in the air. Air initial pressure is $500\,\mathrm{kPa}$ and a detonation driven shock tube produces a Mach 5.3 shock wave with high repeatability. On one hand, schlieren visualizations have shown that decane droplet has comparable behavior than that of water droplet (or decane droplet in pure N_2 atmosphere). On the other hand, chemical reactions sites have been identified thanks to CH^* filtered direct visualization. The main conclusion is that the combustion does not interact dramatically with atomization and breakup processes of the droplet. Chemical reactions mainly occurs in the wake, 5–$7\,\mu\mathrm{s}$ after the shock arrival on the droplet.

References

[1] W. T. Webber, "Spray combustion in the presence of a travelling wave," *Symposium (International) on Combustion*, vol. 8, no. 1, pp. 1129–1140, 1961.

[2] P. Lu and N. Slagg, "Chemical aspects in shock ignition of fuel droplets," *Astronautica Acta*, vol. 17, no. 4-5, pp. 693–702, 1971.

[3] A. V. Pinaev and A. I. Sychev, "Ignition of fuel droplets behind a shock wave front," *Combustion, Explosion and Shock Waves*, vol. 18, no. 6, pp. 682–689, Nov 1982.

[4] D. Hébert, J.-L. Rullier, J.-M. Chevalier, I. Bertron, E. Lescoute, F. Virot, and H. El-Rabii, "Investigation of mechanisms leading to water drop breakup at Mach 4.4 and Weber numbers above 10^5," *SN Applied Sciences*, vol. 2, no. 1, p. 69, Dec 2019.